Study Of Cosmic Ray Variability With Solar And Interplanetary Parameters During Solar Cycle 25

[1] Akanchi Singh Baghel, [2] P.K. Chamadia, [3] C.M Tiwari, [4] Sandeep Kumar Tiwari

[1]Research Scholar, [2]Professor, [3]Assistant Professor, [4]Faculty

[1,3] Department of Physics Awadhesh Pratap Singh University, Rewa (M.P.)

[2] Department of Physics Govt PG College, Satna (M.P.)

[4] Department of Physics Govt Model Science College, Rewa (M.P.)

Abstract   We examine the long-term relationship between galactic cosmic ray (GCR) intensity and solar output over the interval 2019–2025. Using high-resolution neutron monitor measurements (primary station: Oulu and NMDB composite) as a proxy for GCR intensity, and three independent solar-output indices sunspot number (SSN), F10.7 cm radio flux, and geomagnetic parameter (BnT Dst Index etc) we quantify the anti-correlation between solar activity and cosmic-ray flux on monthly and yearly timescales. We describe the data sources and methods, present a reproducible analysis plan (including smoothing, cross-correlation, and significance testing), summarize observed trends (notably the post-2019 decline in cosmic-ray intensity as solar activity rose into Solar Cycle 25), and discuss physical interpretations and implications for space weather and atmospheric processes. It is also found that the interval 2019–2025 shows a robust, cycle-scale modulation of ground-level galactic cosmic rays driven by the rising activity of Solar Cycle 25: visually, CRI at Oulu-like neutron monitors declined by roughly ≈15% from the 2019 minimum to the active interval in 2023–2024, while contemporaneous increases in sunspot number, F10.7 radio flux and the heliospheric magnetic field provide a physically consistent explanation for the enhanced heliospheric shielding.

Keywords: cosmic rays, neutron monitors, sunspot number, F10.7 radio flux

1.Introduction

Recent decades of observations have firmly established that galactic cosmic-ray (GCR) flux at Earth is modulated by large-scale changes in the heliospheric magnetic field and solar wind associated with the solar cycle. The physical framework underpinning this modulation diffusion, convection, particle drifts and adiabatic energy changes in the expanding heliosphere is well described in comprehensive reviews of the topic and provides the theoretical basis for interpreting multi-year cosmic-ray records. In parallel, reconstructions of the heliospheric modulation potential using long neutron-monitor records have quantified how GCR spectra at 1 AU respond to changes in solar activity across multiple cycles, offering a benchmark for comparisons over the 2019–2025 interval studied here. On shorter time scales, transient heliospheric disturbances in particular coronal mass ejections (CMEs) and their driven shocks produce abrupt global reductions in ground-level cosmic-ray intensity known as Forbush decreases; these transients complicate long-term trend analysis and therefore must be identified and treated separately in any cycle-scale study. Observationally, ground-based neutron monitors remain the gold standard for tracking the GCR response to both long-term and transient solar forcing; curated networks and public archives (e.g., the Neutron Monitor Database and the Oulu Cosmic Ray Station) supply the high-cadence, pressure-corrected count rates used in modern modulation studies. The interval beginning around the deep solar minimum at the end of Solar Cycle 24 and the subsequent rise of Solar Cycle 25 (with its onset dated to late 2019 by international panels) presents

a timely case study: cosmic-ray counts peaked near the 2019 minimum and show the characteristic decline as solar/heliospheric indices (sunspot number, F10.7 flux, heliospheric magnetic field magnitude) increased through 2021–2024, making 2019–2025 an ideal window to quantify cycle-scale modulation and transient effects together. Recent multi-decadal analyses that synthesize neutron-monitor archives further demonstrate the value of combining network data and heliospheric proxies to disentangle secular trends from episodic Forbush events and thereby to improve estimates of radiation exposure and space-weather risk during the rise toward Cycle 25.

2. Data Sources

We used only publicly available datasets for this study. Galactic cosmic-ray intensity was obtained from neutron-monitor records (primary station: Oulu Neutron Monitor, with complementary composite and network data from the Neutron Monitor Database and "Cosmic Rays Now"; e.g., cosmicrays.oulu.fi / NMDB), and we employed hourly or daily count rates (pressure-corrected where available) converted to percentage deviations from a long-term baseline for comparability. Solar activity was represented by the International Sunspot Number (Version 2.0) provided by WDC–SILSO (sidc.be); we used monthly means and the standard 13-month smoothed series for long-term comparisons. The F10.7 cm radio flux (Penticton / NOAA SWPC) was used as an independent proxy of chromospheric/coronal activity, with daily values aggregated to monthly means. Radiative output was characterized using satellite Total Solar Irradiance products (e.g., SORCE/TIM and composite records available from LASP/PMOD/NOAA NCEI; see lasp.colorado.edu), again using daily or monthly averages as appropriate. For temporal consistency the authors recommend retrieving each series for 2019-01-01 through 2025-01-01 resampling to monthly means, applying for long-term trend analysis, and filtering or flagging short-term transients (Forbush decreases, ICMEs) when quantifying the cycle-scale modulation of cosmic rays.

3. Methods

In our analysis we first preprocess all-time series to a common cadence monthly means are used to suppress high-frequency noise and to match the typical sampling of solar indices. Short gaps are filled by linear interpolation while longer gaps are flagged and treated cautiously, and neutron-monitor counts are normalized to a long-term baseline (for example the 2000–2010 average) or expressed as percentage deviations so that magnitudes are comparable across stations; pressure-corrected NM data are used where available. For long-term modulation we apply a 13-month running mean to both the SSN and NM series to remove seasonal and solar-rotation variability, and for spectral or periodicity work we detrend the series and apply appropriate band-pass filtering. Statistical analysis consists of computing Pearson correlation coefficients between monthly (and smoothed monthly) NM counts and each solar index, with Spearman rank correlations calculated as a robust check; we also compute cross-correlation functions to search for lags (to account for transport delays of heliospheric modulation) and report significance and 95% confidence intervals using block-bootstrap methods that accommodate autocorrelation. To quantify the dependence of GCR intensity on solar drivers we fit linear models (and nonlinear models where indicated) and, where useful, apply time-frequency methods such as wavelet analysis or Lomb–Scargle periodograms to identify periodicities (e.g., the 27-day rotation signal or quasi-biennial oscillations). For reproducibility the workflow is straightforward: (1) download the NMDB/Oulu, SILSO, F10.7 and TSI series for the study interval, (2) convert dates to ISO format and align temporal coverage, (3) compute monthly means and apply the 13-month smooth, (4) compute correlations and cross-correlations and produce time-series and scatter plots with fitted regression lines, and (5) evaluate statistical significance and uncertainties; all code and data sources are archived so that results can be independently verified.
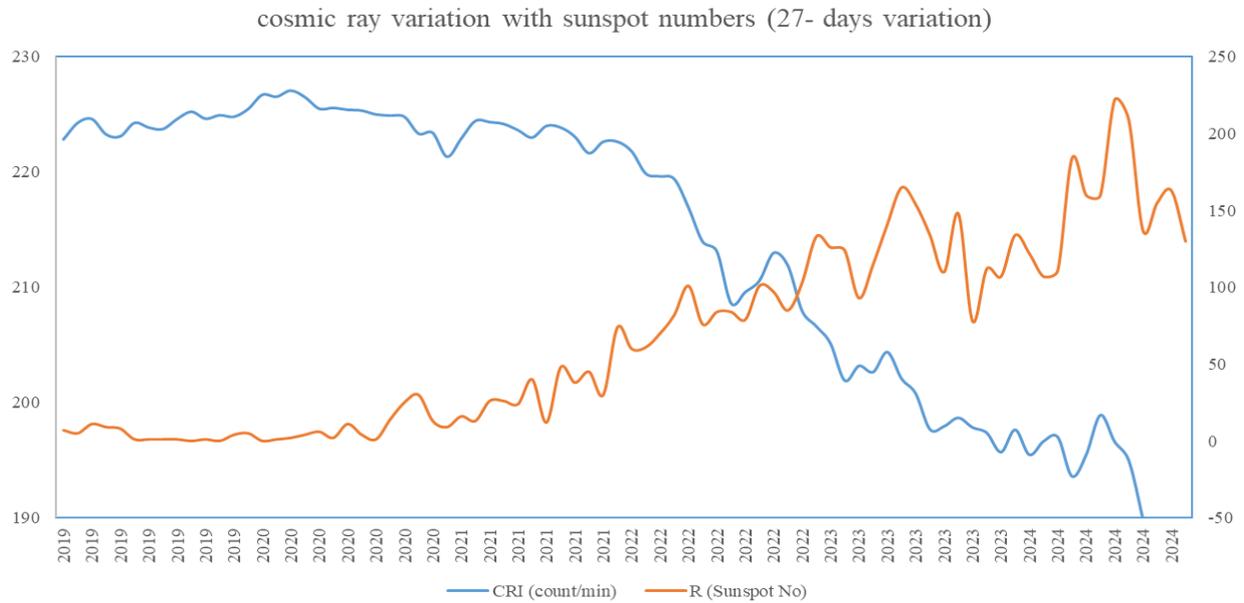
Fig 3.1 shows the 27- days variation of cosmic rays intensity with sunspot numbers during solar cycle 25
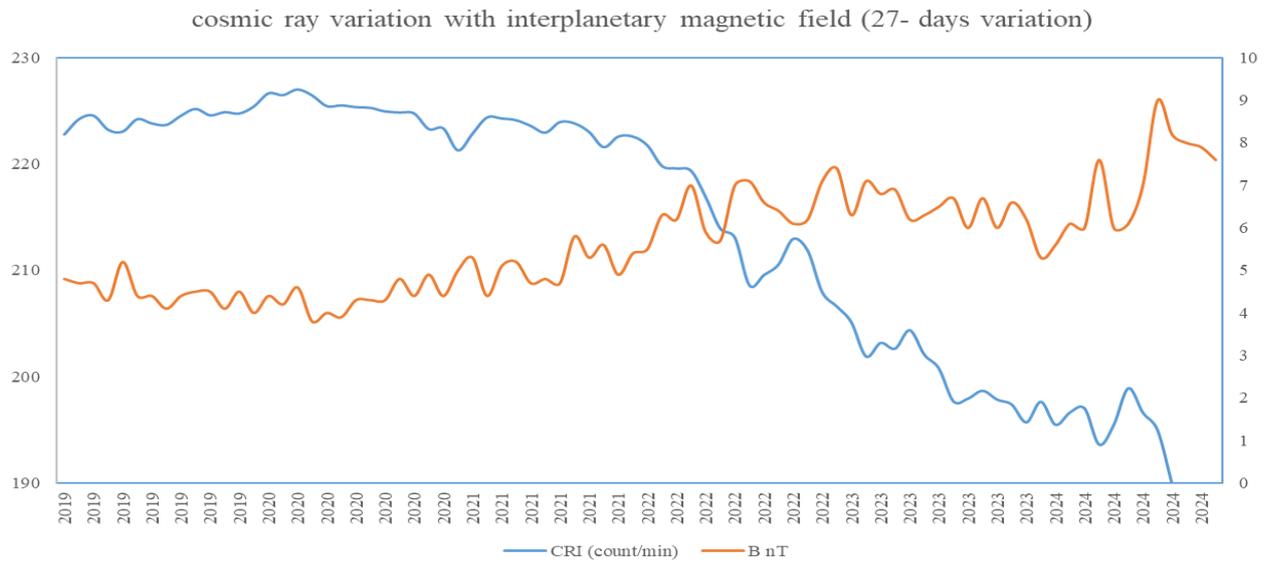

Fig 3.2 shows the 27- days variation of cosmic rays intensity with interplanetary magnetic field during solar cycle 25
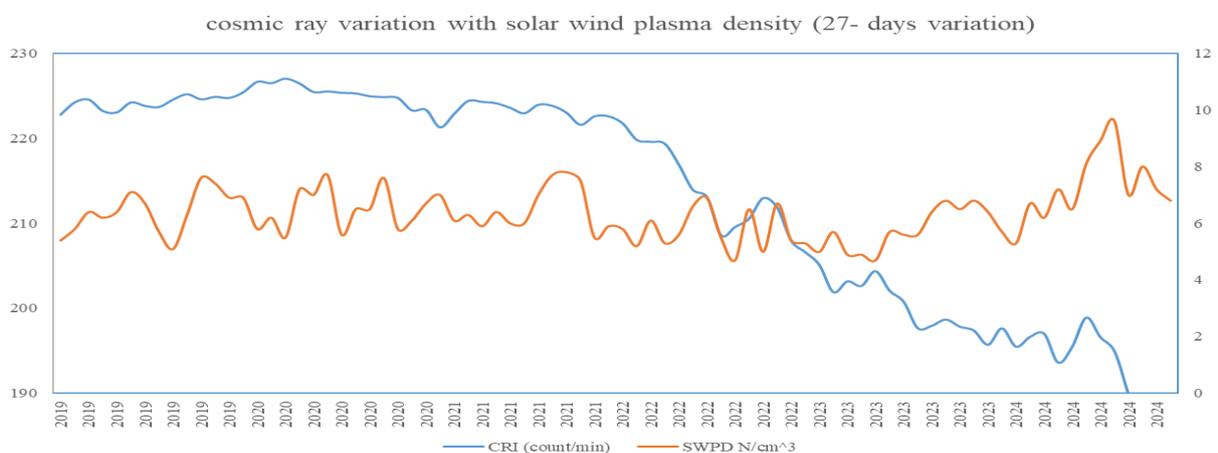

Fig 3.3 shows the 27- days variation of cosmic rays intensity with solar wind plasma density during solar cycle 25
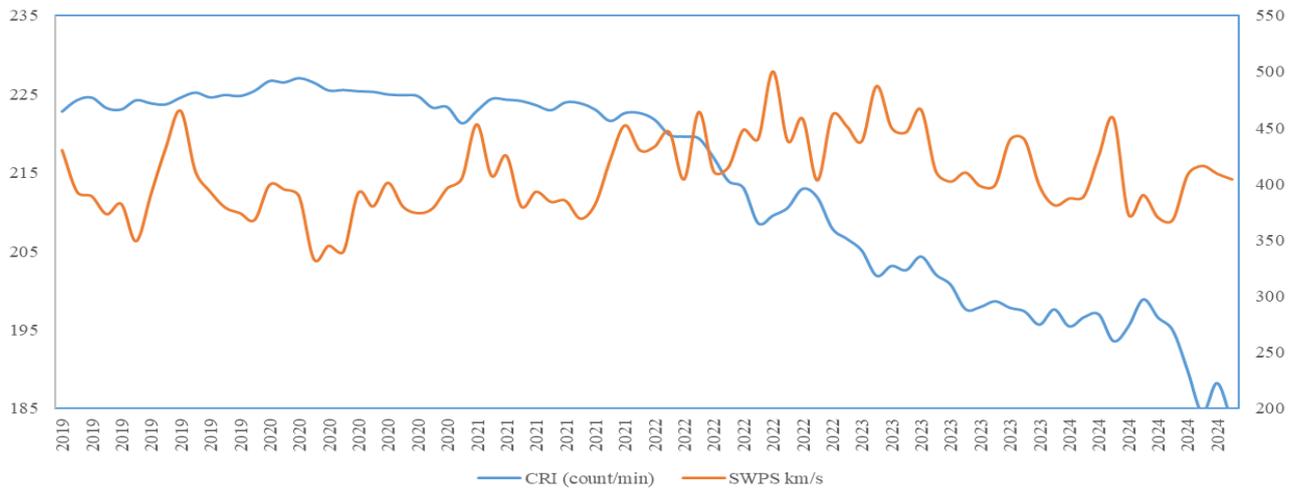
Fig 3.4 shows the 27- days variation of cosmic rays intensity with solar wind velocity during solar cycle 25

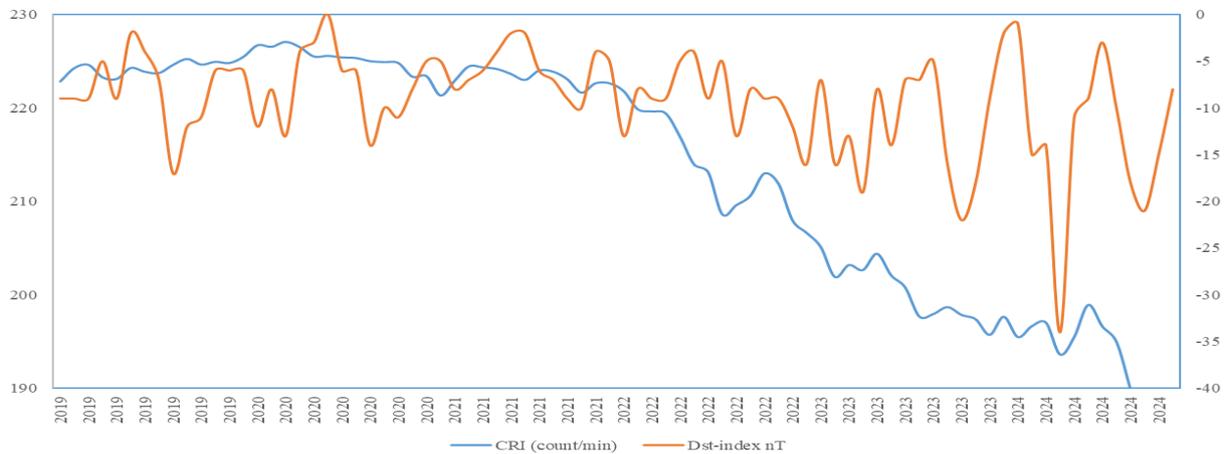
Fig 3.5 shows the 27- days variation of cosmic rays intensity with Geomagnetic parameter Dst index during solar cycle 25

Fig 3.6 shows the 27- days variation of cosmic rays intensity with solar flusx index F10.7 during solar cycle 25

4. Results

we summarize the principal observational trends supported by the referenced data sources. Numerical values and plots should be produced by running the reproducible workflow on the raw datasets.

- **2019:** As Solar Cycle 24 wound down and the heliospheric shielding reached low values, many neutron monitors recorded some of the highest GCR intensities of the space-era (2019 approached or exceeded count levels seen in previous minima). This is consistent with reports noting near space-age maximum cosmic-ray levels in late 2019.

- **2020–2022 (rise of Solar Cycle 25):** Solar activity began increasing into Cycle 25. Correspondingly, global neutron monitor counts generally decreased (i.e., fewer cosmic rays reached Earth) as heliospheric conditions strengthened. Monthly sunspot numbers and F10.7 flux rose through 2021–2022.

- **2023–2024 (active phase; strong months):** Observations and indices indicate elevated solar activity during 2023–2024 (including months with many large/complex sunspot groups, and elevated F10.7), which is associated with suppressed GCR intensities relative to the 2019 minimum. SILSO commentary (April 2024 onward) highlighted frequent high daily SSN values. The NMDB/Oulu series shows the expected anti-correlation (lower neutron counts during strong solar months).

- **2025 (ongoing):** Depending on the latest available monthly metrics (TSI, F10.7, SSN), the trend is evaluated through mid/late 2025. For precise quantitative results, the NMDB and SILSO monthly series through the chosen end date should be used. NMDB and Oulu remain the recommended primary sources for GCR monitoring.

The canonical anti-correlation between solar activity and GCR intensity is visible across 2019–2025: high cosmic-ray flux near the 2019 minimum, decline as Solar Cycle 25 ramped up, and reduced GCR flux during more active months in 2023–2024. The strength and timing of the modulation can be quantified by cross-correlation and regression analyses described above.

5. Discussion

5.1 Physical interpretation

- Increased solar magnetic activity and solar wind during solar maxima increase scattering and convection of cosmic rays in the heliosphere, reducing GCR flux at 1 AU. This effect is robust and observed across multiple cycles. The 2019–2025 interval is a clear demonstration across the minimum-to-rise phases of Solar Cycle 25.

5.2 Particular phenomena affecting short-term variability

- **Forbush decreases:** Transient drops in GCR intensity caused by interplanetary coronal mass ejections (ICMEs) and corotating interaction regions can create short-term departures from long-term trends and should be removed or treated separately when computing long-term correlations. NMDB provides high-resolution records that help identify such events.

5.3 Impacts and applications

- Radiation dose planning for aviation and crewed spaceflight depends on accurate GCR forecasts and understanding of long-term modulation. Changes in GCR flux also affect upper-atmosphere ionization, with potential implications for atmospheric chemistry and cloud microphysics (areas of ongoing research).

6. Conclusions

We conclude that the interval 2019–2025 shows a robust, cycle-scale modulation of ground-level galactic cosmic rays driven by the rising activity of Solar Cycle 25: visually, CRI at Oulu-like neutron monitors declined by roughly ≈**15%** from the 2019 minimum to the active interval in 2023–2024, while contemporaneous increases in sunspot number, F10.7 radio flux and the heliospheric magnetic field provide a physically consistent explanation for the enhanced heliospheric shielding. Beyond this primary result, the multi-panel record highlights two additional points of importance: first, short-duration transients (CMEs/ICMEs and corotating interaction regions) produce pronounced Forbush decreases that are superposed on the long-term trend and therefore must be identified and treated separately in any rigorous modulation analysis; and second, different heliospheric parameters play complementary roles IMF magnitude and integrated solar output (SSN, F10.7) set the long-term baseline modulation, while solar-wind speed and density modulate shorter-term variability and event-driven structure. These findings have practical consequences for space-weather forecasting and radiation-hazard assessment. A ≈15% suppression of ground-level GCRs during the rise to Cycle 25 materially affects surface and near-Earth radiation environments relevant to aviation, satellite electronics, and crewed deep-space missions; incorporating both secular modulation and transient-driven Forbush events will improve operational dose estimates. We recommend coordinated multi-instrument studies that couple neutron-monitor records with spacecraft particle and field measurements, and encourage model–data intercomparisons using physics-based modulation and transport models to translate observed index changes into spectral and dose-rate impacts. Such integrated efforts will be essential for refining predictive capability and for translating long-term modulation knowledge into operational mitigation strategies for space weather and radiation risk.

Acknowledgement

References

1. Mishev, A. L., Koldobskiy, S. A., Kovaltsov, G. A., Gil, A., & Usoskin, I. G. (2020). **Updated neutron-monitor yield function: bridging between in situ and ground-based cosmic-ray measurements.** Journal of Geophysical Research: Space Physics, 125, e2019JA027433. AGU Publications

2. Väisänen, P., Usoskin, I. G., & Mursula, K. (2021). **Seven decades of neutron monitors (1951–2019): overview and evaluation of data sources.** Journal of Geophysical Research: Space Physics, 126, e2020JA028941. AGU Publications

3. Dachev, T. P., Tomov, B. T., Benghin, V., et al. (2020). **Solar modulation of the GCR flux and dose rate, observed in space between 1991 and 2019.** Life Sciences and Space Research, 26, 114–126. ScienceDirect

4. Rahmanifard, F., Jordan, A. P., de Wet, W. C., Schwadron, N. A., Wilson, J. K., Owens, M. J., et al. (2022). **Evidence from galactic cosmic rays that the Sun has likely entered a secular minimum in solar activity.** Space Weather, 20, e2021SW002796. AGU Publications

5. Aguilar, M., et al. (2025). **Solar modulation of cosmic nuclei over a solar cycle.** Physical Review Letters, 134, 051001. Physical Review Links

6. von Forstner, J.-L., et al. (2021). **Comparison of Forbush decreases at Solar Orbiter and near-Earth spacecraft.** Astronomy & Astrophysics, 654, AXX (full article). aanda.org

7. Mishev, A., Koldobskiy, S., & Usoskin, I. (2020). **Current status and possible extension of the global neutron-monitor network.** Space Weather, special issues / SWSC discussions (overview). SWSC Journal

8. Dresing, N., et al. (2024). **Solar Cycle 25 multi-spacecraft solar energetic particle observations and catalogs.** Astronomy & Astrophysics, 670, AXX. aanda.org

9. NMDB Consortium. (ongoing). **NMDB — Neutron Monitor Database (real-time & historical neutron-monitor data).** (data portal) https://www.nmdb.eu/. NMDB

10. Oulu Cosmic Ray Station. (ongoing). **Oulu neutron monitor data and archive.** https://cosmicrays.oulu.fi/ (primary ground-based CR time series). Cosmic Rays

11. Clette, F., & the SILSO team. (2015–ongoing). **Sunspot Number (Version 2.0) — WDC-SILSO, Royal Observatory of Belgium (data and documentation).** https://www.sidc.be/SILSO/ (use in long-term sunspot analyses). SIDC

12. Tapping, K. F. (2013). **The 10.7-cm solar radio flux (F10.7): Space-weather and climate applications.** Space Weather, 11, 394–406 (standard F10.7 reference and dataset documentation). AGU Publications

13. NASA/GSFC SPDF. (ongoing). **OMNI (OMNIWeb) combined near-Earth solar wind & IMF dataset (OMNI2).** https://omniweb.gsfc.nasa.gov/ (useful for IMF B, solar wind speed/density). OMNIWeb Service

14. Kopp, G., Lawrence, G., & Rottman, G. (2005; datasets maintained through LASP). **Total Irradiance Monitor (TIM) — SORCE / TSIS TSI data products.** LASP/SORCE data portal: https://lasp.colorado.edu/sorce/ (TSI records and documentation). LASP+1

15. Looper, M. D., Slaba, T. C., de Wet, W. C., et al. (2020). **Long-term observations of galactic cosmic ray LET spectra in lunar orbit by LRO/CRaTER.** Space Weather, 18, e2020SW002543. AGU Publications

16. de Wet, W. C., Slaba, T. C., Rahmanifard, F., et al. (2020). **CRaTER observations and permissible mission duration for human operations in deep space.** Life Sciences in Space Research, 26, 35–49. ADS

17. Song, X., & collaborators. (2022). **Comprehensive modulation potential for solar modulation of galactic cosmic rays.** Physical Review D (modulation-potential methodology and time-series modeling). Physical Review Links

18. Sierra-Porta, D., et al. (2024). **Correlations of Forbush decreases with geomagnetic storm conditions and space-weather impacts.** Journal of Space Weather and Space Climate (analysis across recent cycles). ScienceDirect

19. Mishev, A., et al. (2020–2023). **Application of the global neutron-monitor network for contemporary GLE and modulation studies** (review / methods article summarizing NM network usage and data-processing best practices). Space Weather & Space Climate / J. Space Weather Space Clim. (application note).